applied sciences

MDPI

Article

Research on the Effects of Two-Sided Ground Surcharge/Unloading on Existing Shield Tunnels

Gang Wei [1,2,3,4], Pengfei Xiang [5,6,*], Haibo Jiang [5,*], Di Sun [7], Fengjun Xu [6] and Huifang Guo [6]

1 Department of Civil Engineering, Zhejiang University City College, Hangzhou 310015, China
2 Key Laboratory of Safe Construction and Intelligent Maintenance for Urban Shield Tunnels of Zhejiang Province, Hangzhou 310015, China
3 Zhejiang Engineering Research Center of Intelligent Urban Infrastructure, Hangzhou 310015, China
4 College of Civil Engineering and Architecture, Zhejiang University, Hangzhou 310058, China
5 College of Water Conservancy & Architectural Engineering, Shihezi University, Shihezi 832000, China
6 Department of Architectural Engineering, Zhejiang Tongji Vocational College of Science and Technology, Hangzhou 311200, China
7 Capital Construction Department, Jiangsu Open University, Nanjing 210037, China
* Correspondence: z20120190803@zjtongji.edu.cn (P.X.); klaud618@shzu.edu.cn (H.J.)

Abstract: For the effect of two-sided sudden surcharge/unloading on existing shield tunnels, an indoor dimensional reduction model test was conducted at a scale of 1:15.5, measuring the ground settlement, lateral convergence of the shield tunnel, and additional surrounding pressure after changing the location and soil quality of surcharge/unloading, and an analysis was carried out. The results showed that the location of the maximum transverse convergence value of the existing shield tunnel is related to the position of the surcharge; when surcharging on both sides of the tunnel, as the position of the left surcharge's offset increases from 0.2 m to 0.6 m, the transverse convergence value of the tunnel first increases and then becomes smaller; the ground settlement value of each measurement point in the unloading process also increases and then becomes smaller. The settlement value of each measurement point first increases and then decreases, and the alleviation effect of unloading on ground settlement is not obvious; after surcharge on one side of the tunnel, if the other side continues to surcharge, it will lead to a continued increase in the surrounding pressure. Unloading can effectively reduce the additional surrounding pressure of the tunnel, but the additional surrounding pressure cannot be immediately and completely eliminated; compared with dry sand, the maximum value of lateral convergence of the tunnel in wet sand is significantly decreased, and the peak value of ground settlement on both sides is not significant; when both sides are surcharged to 172 kg, the additional soil pressure of the tunnel's subsoil shows three peaks, one of which occurs at measurement point 4 at the bottom of the tunnel, which may be due to the occurrence of stress concentration at the location.

Keywords: two-sided surcharge/unloading; shield tunnel; location; soil

check for updates

Citation: Wei, G.; Xiang, P.; Jiang, H.; Sun, D.; Xu, F.; Guo, H. Research on the Effects of Two-Sided Ground Surcharge/Unloading on Existing Shield Tunnels. *Appl. Sci.* **2022**, *12*, 12494. https://doi.org/10.3390/app122312494

Academic Editors: Jong Wan Hu and Daniel Dias

Received: 25 October 2022
Accepted: 5 December 2022
Published: 6 December 2022

1. Introduction

The subway has become an important and indispensable vehicle in many big cities with the promotion of large-scale urbanization in China, and there is a trend of developing and constructing multilevel subway superstructures such as commercial, office, and residential buildings in the upper space of the subway to make full use of the land resources in the core of the city. With the construction of the subway superstructure, surcharge/unloading will inevitably occur on the left and right sides above the existing shield tunnel, adversely affecting the tunnel and the surrounding soil. Therefore, it is important to study the impacts of surcharge/unloading on both sides of the existing tunnel below.

To date, several domestic and foreign scholars have conducted studies on the influence of surcharge/unloading above existing shield tunnels on the tunnel and the surrounding soil, including field measurement methods [1–5], model test methods [6–12], limit element analysis methods [13–21], theoretical calculation methods [22–31], etc., among which the model test methods can simulate the actual engineering situation to the greatest extent, and the measured results are relatively accurate and reliable. Xiang Pengfei et al. [6] studied the impacts of surcharge and excavation directly above a tunnel in soft clay on the ground settlement and the existing shield tunnel below via model tests. Wei Gang et al. [7] studied the influence of the surcharge above a tunnel in sand on the lateral and vertical deformation of the shield tunnel through model tests. Zhang Shuming [8] studied the influence of surcharge above a tunnel in sand on the additional confining pressure of the shield tunnel through model tests. Fayun Liang et al. [9] studied the effect of surcharge position on the lateral deformation of shield tunnels in different soft and hard strata by means of comparative tests. Sun Huasheng et al. [10] studied the deformation mechanism of shield tunnels under different surcharge sizes, surcharge areas, and tunnel depths by means of indoor model testing, and also verified the reliability of the model test by means of finite element simulation. Wu Qing et al. [11] studied the deformation mechanism of shield tunnels by means of indoor model tests, with emphasis on the buried depth and location of the tunnel. Atkinson J.H. et al. [12] investigated the stability changes of a tunnel under different surcharge and support conditions by means of model tests and theoretical calculations. The existing model test studies were all conducted for surcharge/unloading on one side of the existing shield tunnel, while there have been few studies of surcharge/unloading on both sides above existing shield tunnels, and the location of the surcharge/unloading and soil determine the adverse effects of surcharge/unloading on the tunnel and the surrounding soil. Therefore, it is necessary to adopt the model test method to consider the effects of two-sided surcharge/unloading, surcharge/unloading position, and soil changes on the existing shield tunnel and the surrounding soil.

A large-scale indoor model test was conducted in this study to determine the influence of surcharge/unloading position and soil changes on the lateral convergence, additional surrounding pressure, additional soil pressure, and ground shift of an existing shield tunnel in the event of surcharge/unloading on two sides of the shield tunnel, in order to obtain a better understanding of the possible adverse effects of surcharge/unloading on two-sided subway superstructure construction.

2. Indoor Model Test

2.1. Test Materials and Equipment

The dry sand used in the test was sea sand sieved through an 18-mesh (about 1 mm) sieve and exposed to the Sun, and the mechanical properties of the treated dry sand are shown in Table 1 below. The wet sand used was the treated dry sand mixed with water, with a moisture content of about 8.23%.

Table 1. Physical and mechanical indices of dry sand.

Density (g)	Water Content (%)	Angle of Internal Friction (°)	Cohesive Force (kPa)	Compression Modulus (MPa)
1.495	0.23	29	0	2.89

The model tunnel used for the test is shown in Figure 1. The model tunnel has 23 rings; each ring has 5 pieces of curvature of 67.5° and 1 piece of curvature of 22.5° of the Plexiglas tube sheet through the bolt connection; the length is 1.78 m, the diameter is 0.4 m, and the thickness is 22.5 mm. Using a scale of 1:15.5, corresponding to a total of 27.6 m of a tunnel with 23 ring tube sheets as the object of study, the outer diameter of the tunnel is 6.2 m, the tunnel tube sheet ring width is 1.2 m, and the thickness of the tube sheet is 0.348 m. The similarity constants of the indoor model test are shown in Table 2, the geometric parameters and material properties of the tunnel model are shown in Table 3, and the geometric parameters and material properties of the tunnel connection bolts are shown in Table 4.

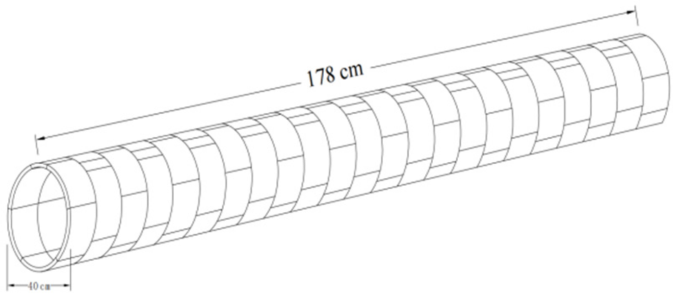

Figure 1. Model tunnel used for the test.

Table 2. Similarity constants for the indoor model tests.

Physical Quantities	Similarity Relationship	Similarity Constants	Physical Quantities	Similarity Relationship	Similarity Constants
Geometric dimensions	Basic quantities	15.5	Bending moment	$C_M = C_E \times {C_L}^3$	62,375
Pressure	Basic quantities	16.75	Shaft force	$C_N = C_E \times {C_L}^2$	4024
Strain	C_ε	1	Bending stiffness	$C_{EI} = {C_L}^4$	57,720
Stress	$C_\sigma = C_E$	16.75	Axial stiffness	$C_{EA} = {C_L}^3$	3724
Displacement	$C_\delta = C_\iota$	15.5	Shear stiffness	$C_{GA} = {C_L}^3$	3724

Table 3. Geometric parameters and material properties of the tunnel model.

	Outer Diameter of the Tube Sheet/m	Tube Sheet Inner Diameter/m	Tube Sheet Thickness/m	Ring Width/m	Modulus of Elasticity of the Tube Sheet/MPa	Poisson's Ratio
Prototype	6.200	5.504	0.348	1.200	34,500	0.2
Model	0.400	0.356	0.022	0.077	2060	0.3

Table 4. Geometric parameters and material properties of the tunnel connection bolts.

	Bolt Length/m	Bolt Diameter/m	Number of Bolts/m	Bolt Modulus of Elasticity/MPa	Poisson's Ratio of Bolts
Prototype	0.400	0.030	17	200,000	0.3
Model	0.027	0.002	6	33,800	0.32

The dimensions of the model box used for the test were 1.8 m × 1.8 m × 1.5 m, as shown in Figure 2.

Figure 2. Model box.

2.2. Test Conditions

For the existing shield tunnel in two-sided surcharge/unloading, to determine the effects of surcharge/unloading position and soil changes on the existing shield tunnel and the surrounding soil, this study conducted a total of four groups of indoor model tests, with each group of tests in the surcharge/unloading order: the left area by level surcharge; the right area by level unloading; the left area by level unloading; and the right area by level unloading. The specific test conditions are shown in Table 5 below.

Table 5. Test conditions.

Test Number	Left Side Surcharge Center Position	Surcharge Area (cm^2)	Left Surcharge Size	Right Surcharge Size	Right Center Surcharge	Total Thickness of Soil Layer	Tunnel Depth	Test Sand
1	0.2 m	40 × 40	0 to 172.0 kg	0 to 172.0 kg	0.4 m	1.2 m	0.6 m	Dry sand
2	0.4 m	40 × 40	0 to 172.0 kg	0 to 172.0 kg	0.4 m	1.2 m	0.6 m	Dry sand
3	0.6 m	40 × 40	0 to 172.0 kg	0 to 172.0 kg	0.4 m	1.2 m	0.6 m	Dry sand
4	0.4 m	40 × 40	0 to 172.0 kg	0 to 172.0 kg	0.4 m	1.2 m	0.6 m	Wet sand

In test conditions 1~4, earth pressure boxes No. 1~8 were uniformly set at the central section of the tunnel to measure the additional surrounding pressure of the tunnel. Five pairs of horizontal displacement gauges were set from the central part of the tunnel, numbered 1~5 in order from the middle to the edge of the tunnel, and the interval of the adjacent horizontal displacement gauges was 0.154 m, 0.154 m, 0.231 m, and 0.231 m, in order, for measuring the lateral convergence. Displacement gauges No. 1~7 were set transversely on the ground at a horizontal distance of 0.4 m from the center of the tunnel, and the interval of the adjacent displacement gauges was 0.2 m, which was used to measure the ground settlement. In Case 4, additional soil pressure boxes 1#~7# were set up in the soil layer where the tunnel bottom was located to measure the tunnel's bottom soil pressure, where soil pressure box 4# is the same as soil pressure box 5# used to measure the tunnel perimeter pressure. The layout of the specific test is shown in Figure 3.

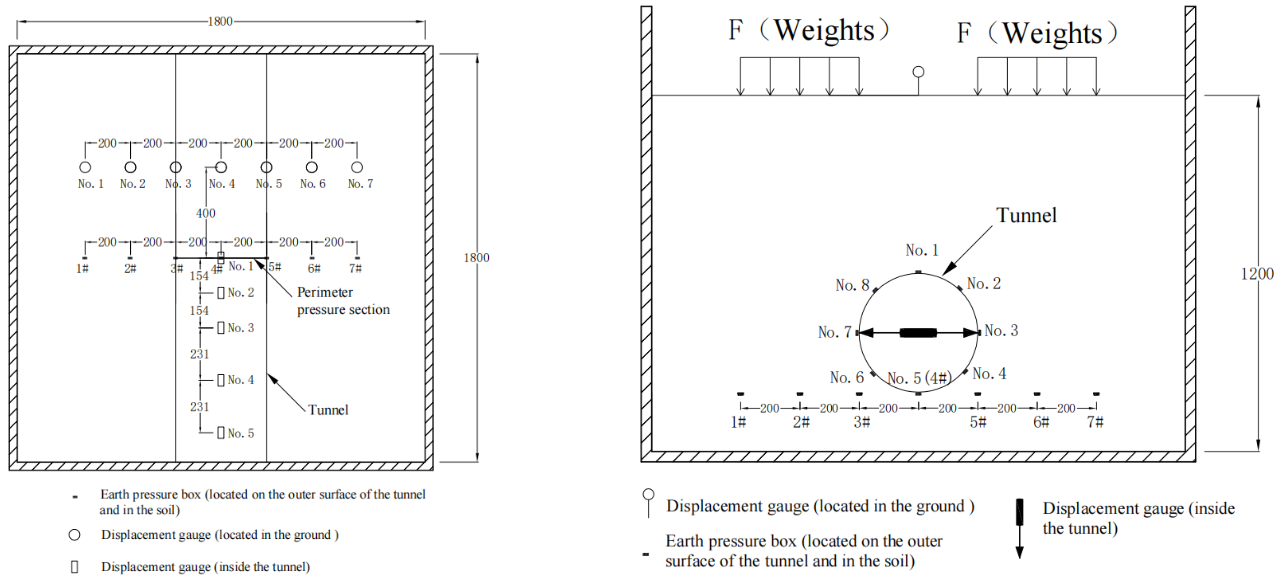

(**a**) (**b**)

Figure 3. *Cont.*

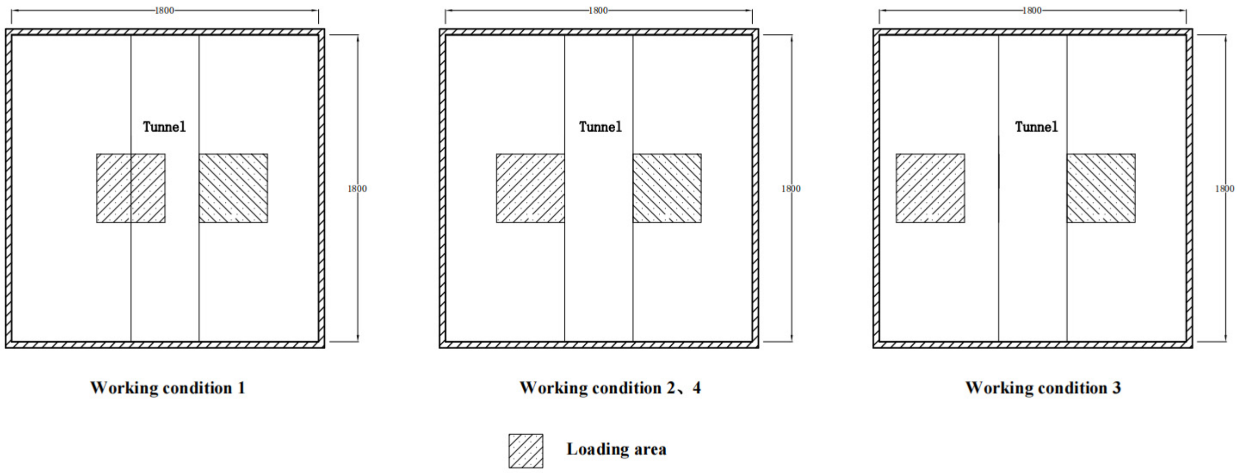

(**c**)

Figure 3. Schematic diagram of the test arrangement (unit: mm): (**a**) Plan view of measurement point arrangement. (**b**) Section view of measurement point arrangement. (**c**) Surcharge schematic diagram.

2.3. Test Steps

(1) First, the shift meter for measuring the lateral convergence value of the tunnel and the earth pressure box for measuring the tunnel pressure are installed at the designated position of the model tunnel, and then the model tunnel is lifted to the designated position of the model box, after which the sand is loaded into the model box for the test at 0.1 m/layer. If under Cases 1~3, this is performed until the total thickness of the soil layer reaches 1.2 m, and then the shift meter for measuring the ground settlement is installed on the surface of the sand. Then, the shift meter and the earth pressure box are connected to the resistive strain gauge and, finally, the sand is left to stand for more than 24 h. In the case of Case 4, the earth pressure box for measuring the earth pressure at the bottom of the central section of the tunnel is installed at 0.2 m, and the rest of the operation is the same as that of Cases 1~3. The layout of the shift meter for measuring the ground settlement on the sand surface is shown in Figure 4.

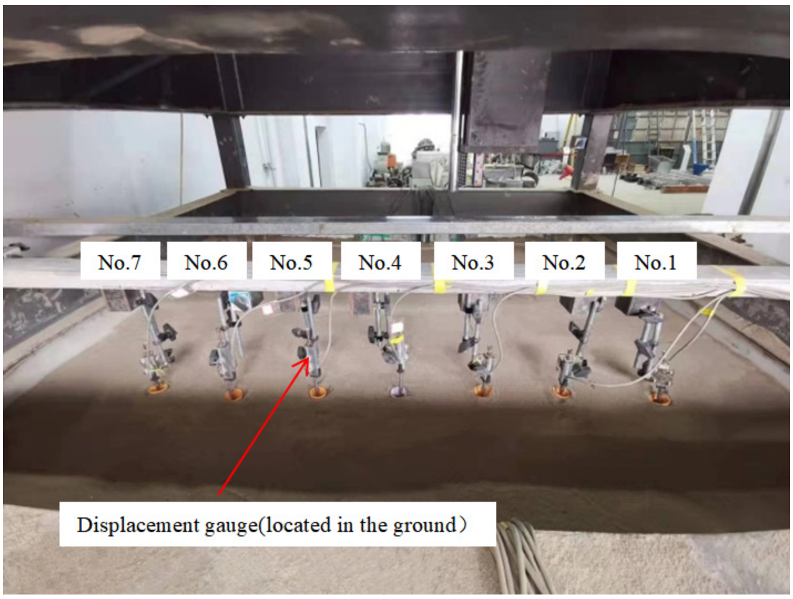

Figure 4. Arrangement of displacement gauges for measuring ground settlement on the sand surface. (The label of displacement meter is from the 1st to the 7th).

(2) Set all displacement gauges and earth pressure box readings to zero, put the 0.4 m × 0.4 m pressure plate in the designated position on the left side in Figure 3c according to the test condition, and surcharge 34.4 kg (including the weight of pressure plate), 68.8 kg, 103.2 kg, 137.6 kg, and 172.0 kg on the pressure plate with corresponding weights step by step. Then, put the 0.4 m × 0.4 m pressure plate in the designated position on the right side in Figure 3c, and surcharge 34.4 kg (including the weight of the pressure plate), 68.8 kg, 103.2 kg, 137.6 kg, and 172.0 kg with weights on the pressure plate step by step. Next, unload the weights on the left side of the pressure plate to 137.6 kg, 103.2 kg, 68.8 kg, 34.4 kg, and 0 kg. Finally, unload the weights on the right side of the pressure plate to 137.6 kg, 103.2 kg, 68.8 kg, 34.4 kg, and 0 kg. The duration of each level of surcharge and unloading is 0.5 h, and the shift meter and earth pressure box read the data every 1 s during the whole surcharge and unloading process.

3. Results and Discussion

3.1. The Impact of Dry Sand in Two-Sided Surcharge/Unloading on the Tunnel Below

3.1.1. The Effect on Lateral Convergence

The lateral convergence on the left side of the tunnel with an eccentric surcharge of 172 kg and on the right side without surcharge is shown in Figure 5; the lateral convergence of the tunnel under the two-sided eccentric surcharge of 172 kg is shown in Figure 6. The lateral convergence deformation of each measurement point of the tunnel in each surcharge stage in Case 1 is shown in Figure 7. The transverse convergence of each measurement point with the surcharge is shown in Figure 8. A positive value of the convergence represents a lateral increase in the tunnel section, while a negative value represents a lateral decrease in the tunnel section.

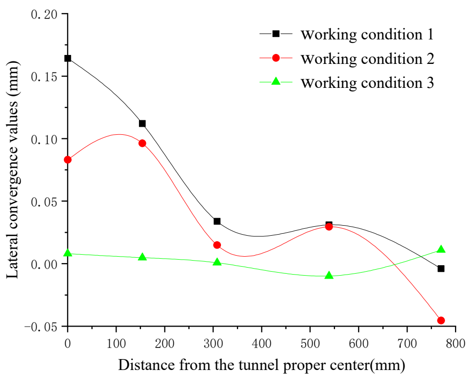

Figure 5. Change in the lateral convergence of each measurement point of the tunnel when the surcharge (172 kg) is only on the left side.

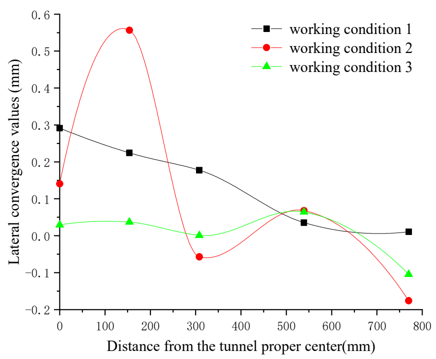

Figure 6. Change in the lateral convergence of each measurement point of the tunnel when the surcharge (both 172 kg) is on two sides.

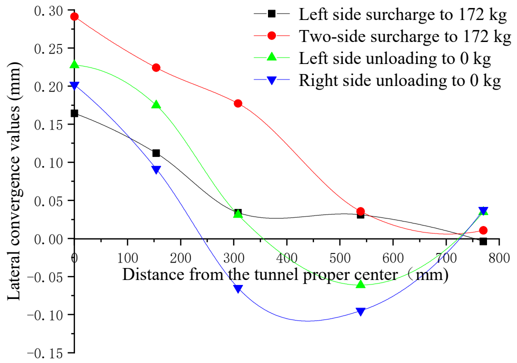

Figure 7. Transverse convergence deformation of each measurement point in each surcharge stage in Case 1.

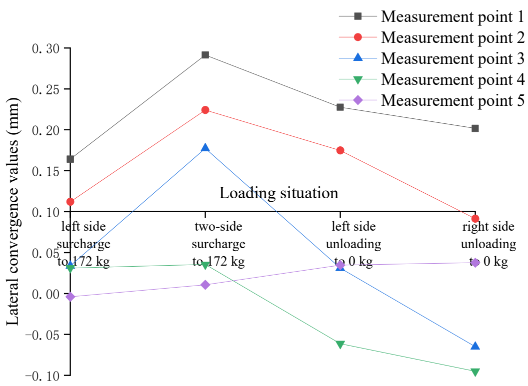

Figure 8. Transverse convergence variation of each measurement point with surcharge in Case 1.

According to Figures 5 and 6, the following can be seen:

(1) In Cases 1~3, the tunnel's maximum transverse convergence values occur when the eccentric surcharge is 172 kg on two sides of the tunnel, but the maximum transverse convergence value for Case 1 occurs at measurement point 1 (right in the middle of the tunnel), while Cases 2 and 3 occur at measurement point 2, due to the different locations of the loads on the two sides of the tunnel, resulting in different combined forces of the loads acting on the tunnel on two sides.

(2) The maximum lateral convergence value of the tunnel in Case 1 is 0.2914 mm, the maximum lateral convergence value of the tunnel in Case 2 is 0.5562 mm, and the maximum lateral convergence value of the tunnel in Case 3 is 0.0368 mm, indicating that when the surcharge is applied on two sides of the tunnel, as the position of the left surcharge's offset increases from 0.2 m to 0.6 m, the lateral convergence value first increases and then becomes smaller, and decreases rapidly after the surcharge offset reaches a certain degree.

(3) Case 2 is a symmetric surcharge on two sides; after the eccentric surcharge on the left side is 172 kg, when the right side continues to surcharge to 172 kg, it is equivalent to the total load increasing by a factor of 1, but the local lateral convergence value of the tunnel increases by several times, which is extremely harmful to the tunnel.

According to Figures 7 and 8, the following can be seen:

(1) When the surcharge is on two sides under dry sand soil, unloading on either side can effectively reduce the lateral convergence value of the tunnel. Taking measurement point 1 as an example, after unloading the surcharge on two sides, the lateral convergence value decreases from the maximum 0.2914 mm to 0.2017 mm, representing a reduction of 30.6%.

(2) In the process of unloading a two-sided surcharge under dry sand soil, the lateral convergence value of the tunnel is negative, indicating that the tunnel section becomes laterally smaller at this time, which may be due to the redistribution of soil stresses during the unloading process, making the tunnel's lateral convergence recover "excessively".
(3) The transverse convergence of measurement point 5 is less regular, because measurement point 5 is the farthest from the surcharge, and the transverse convergence value is small, while there is an obvious "boundary effect" near the edge of the model box.

The transverse convergence deformation of measurement point 1 (in the middle of the tunnel) at each surcharge stage in Case 1 can be seen in Figure 9, where θ_{sand} represents the pressure diffusion angle.

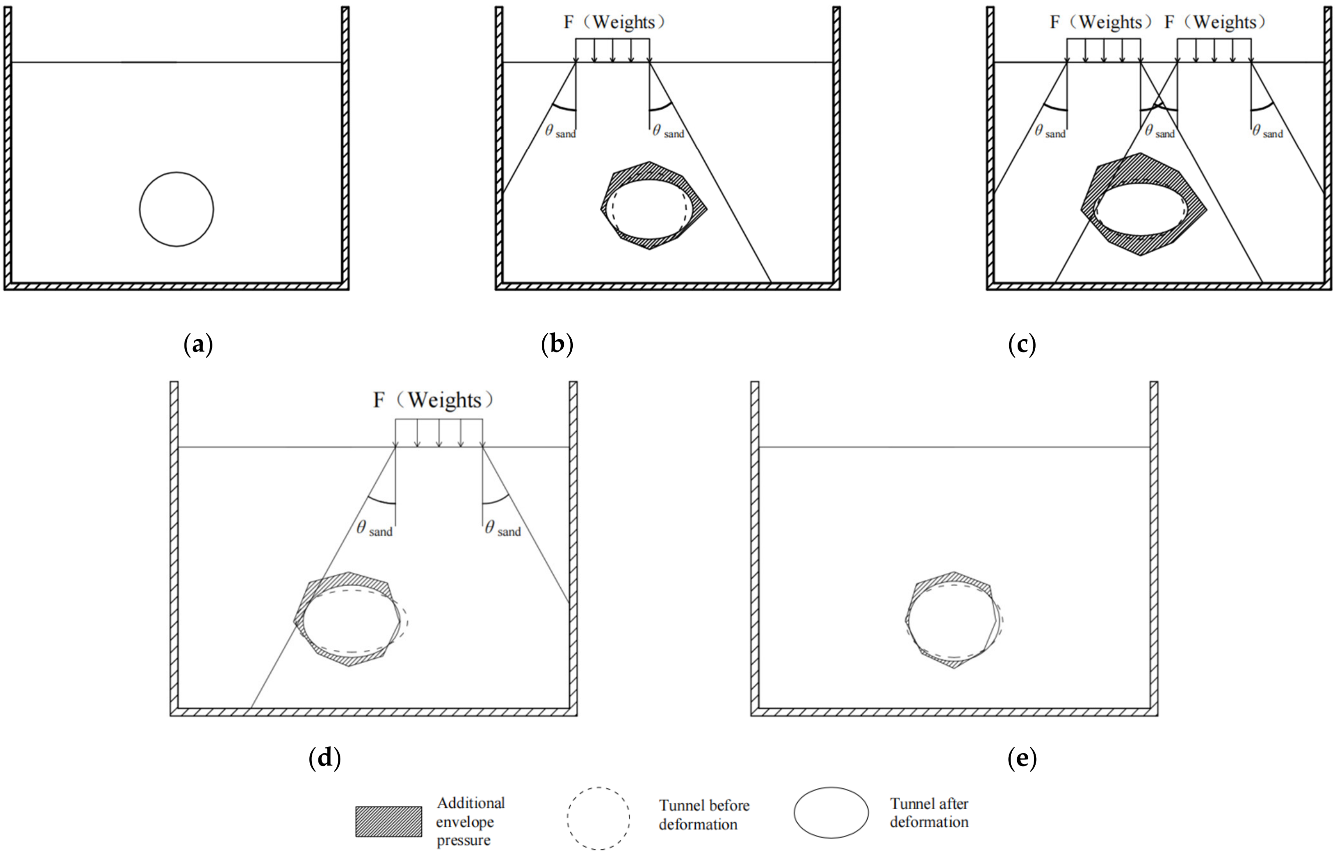

Figure 9. Schematic diagram of the change in the central section of the tunnel at each surcharge stage of Case 1: (**a**) No surcharge. (**b**) Left-sided surcharge 172 kg. (**c**) Two-sided surcharge to 172 kg. (**d**) Unloading to 0 kg on the left side. (**e**) Unloading to 0 kg on two sides.

3.1.2. Effect on Ground Settlement

The variations in ground shift under different surcharges for Cases 1~3 are shown in Figures 10–12, where a positive value of the ground shift represents augmentation and a negative value represents settlement.

Combining Figures 10–12, we can see that the following:

(1) As the position of the left surcharge's offset increases from 0.2 m to 0.6 m, the peak of the left ground settlement also shifts, and the peak of the left settlement decreases from 0.9815 mm to 0.5925 mm in the process of the offset, which is mainly due to the change in the position of the left surcharge's offset, resulting in the boundary effect becoming more and more obvious.
(2) The amount of settlement at each measurement point of the ground first increases and then decreases during the unloading process, and the effect of unloading on the

mitigation of ground settlement is not obvious, because the soil is still consolidating during the unloading process, causing the maximum amount of ground settlement. This is because during the unloading process, the soil is still consolidating, which leads to the maximum amount of ground settlement lagging behind.

(3) The peak of the ground settlement on the left and right sides always occurs when the right surcharge is 172 kg and the left surcharge is finished unloading; the final peak of the ground settlement on the right side during the whole surcharge/unloading process is always larger than the final peak of the ground settlement on the left side. This may be related to the sequence of surcharge/unloading.

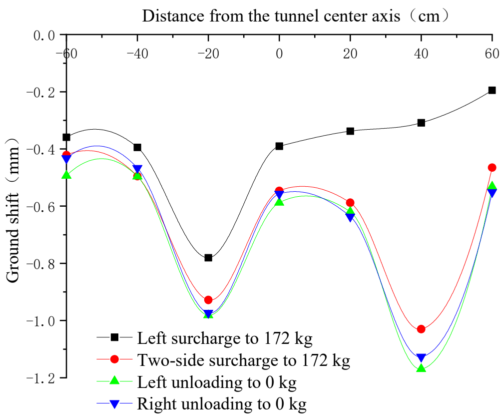

Figure 10. Variation in ground shift under different surcharges for Case 1.

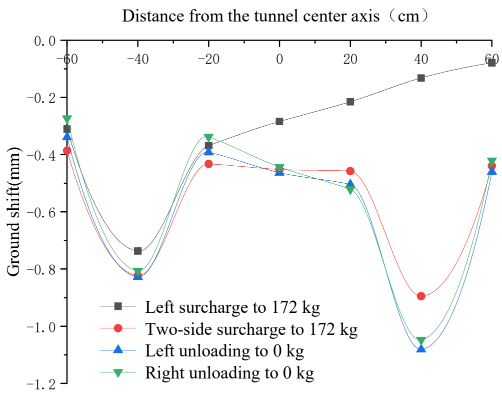

Figure 11. Variation in ground shift under different surcharges for Case 2.

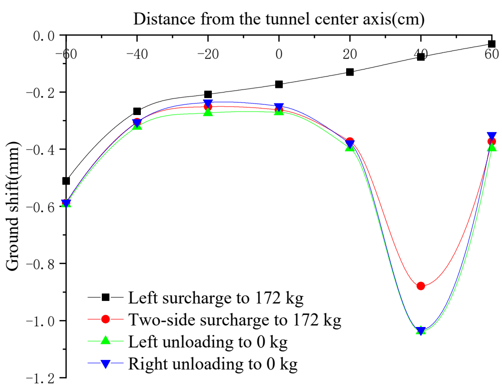

Figure 12. Variation in ground shift under different surcharges for Case 3.

3.1.3. Influence on Additional Surrounding Pressure

The changes in the additional surrounding pressure in the central section of the tunnel for Cases 1~3 are shown in Figures 13–15, where positive values of additional surrounding pressure represent the pressure while negative values represent the tension.

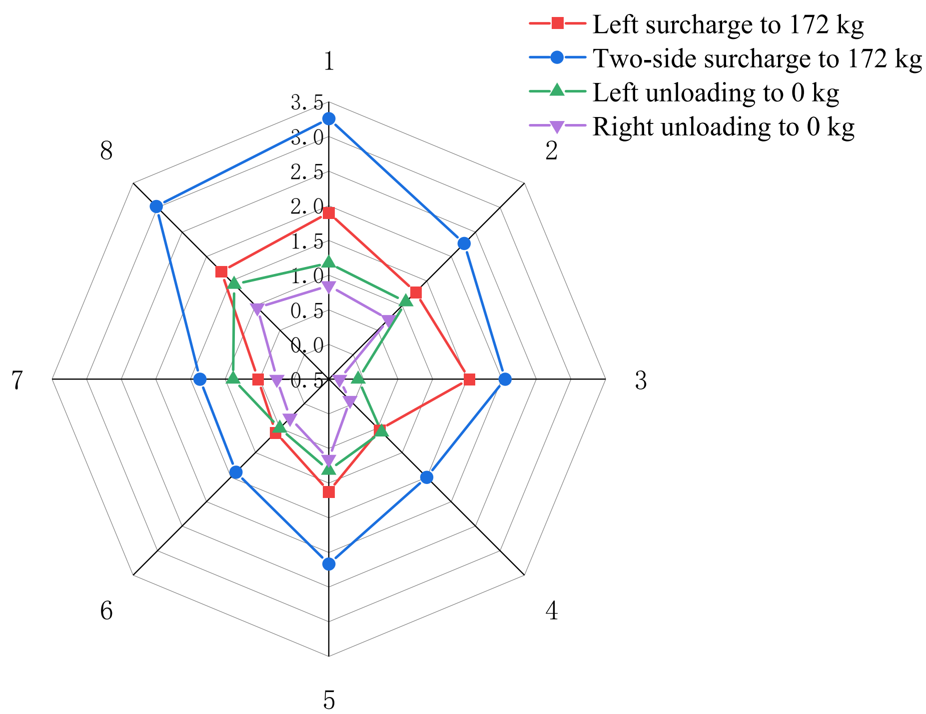

Figure 13. Variation in additional surrounding pressure under different surcharges for Case 1 (unit: kPa).

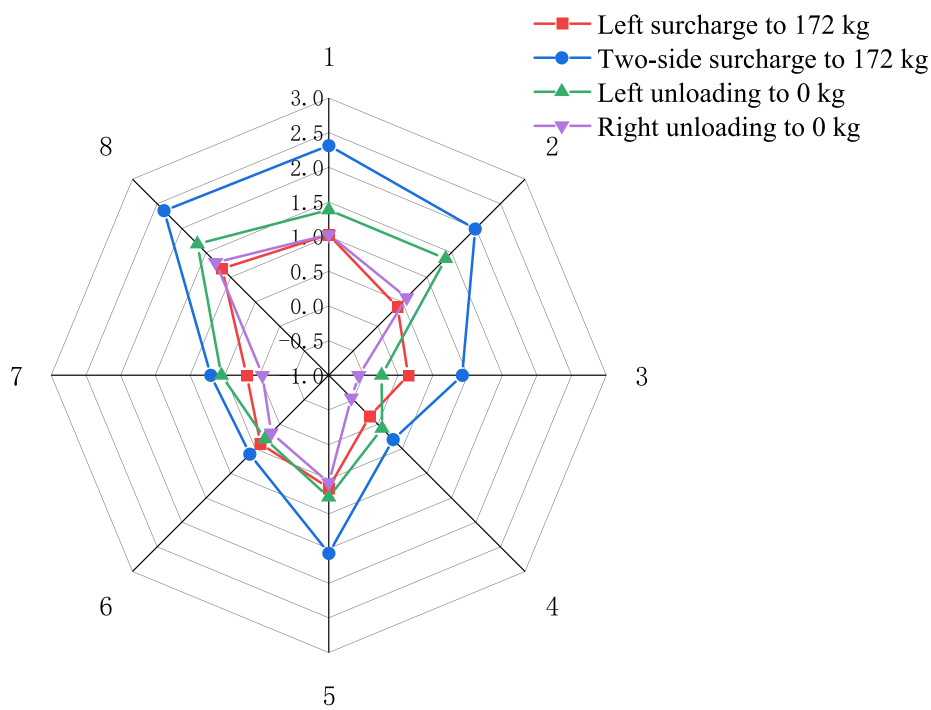

Figure 14. Variation in additional surrounding pressure under different surcharges for Case 2 (unit: kPa).

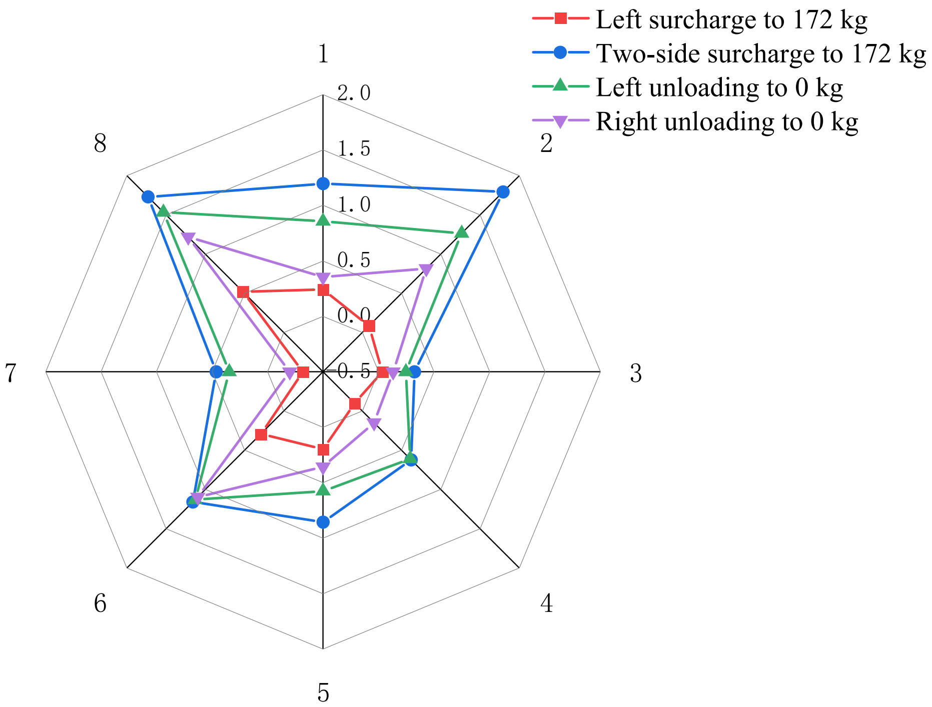

Figure 15. Variation in additional surrounding pressure under different surcharges for Case 3 (unit: kPa).

Combining Figures 13–15, the following can be seen:

(1) As the position of the left surcharge offset increases from 0.2 m to 0.6 m, the additional surrounding pressure of the tunnel decreases sharply. Taking point 1 as an example, with a left surcharge of 172 kg, the additional surrounding pressure decreases from 1.9003 kPa to 0.2410 kPa when the left surcharge's offset position increases from 0.2 m to 0.6 m, which is 87.3%; with the left and right surcharge of 172 kg, the additional surrounding pressure decreases from 3.2576 kPa to 0.3545 kPa when the left surcharge's offset position increases from 0.2 m to 0.6 m, representing a decrease of 89.1%.

(2) After surcharge on one side of the tunnel, if the other side continues to surcharge, it will cause the surrounding pressure to continue to increase, and when the surcharge on two sides reaches 172 kg, the local additional surrounding pressure of the tunnel increases by more than 100%, which is extremely harmful to the tunnel.

(3) In dry sand, unloading can effectively reduce the additional surrounding pressure of the tunnel, but it will not eliminate the additional surrounding pressure immediately; after unloading is completed, the additional surrounding pressure will still exist in most of the tunnel to some extent. The more distant the surcharge location, the higher the residual proportion of additional pressure.

The changes in additional pressure in the center of the tunnel in each surcharge stage in Case 1 are shown in Figure 9.

3.2. Influence of Two-Sided Surcharge/Unloading on the Tunnel Below Using Wet Sand

3.2.1. Influence on Lateral Convergence

The variation in the lateral convergence of each measurement point in the tunnel under different surcharges in Case 4 is shown in Figures 16 and 17, while the variation in the lateral convergence of the 1st and 2nd measurement points with the surcharge in Case 2 and Case 4 is shown in Figure 18. A positive value of transverse convergence means that the tunnel's transverse section becomes larger, while a negative value means that the tunnel's transverse section becomes smaller.

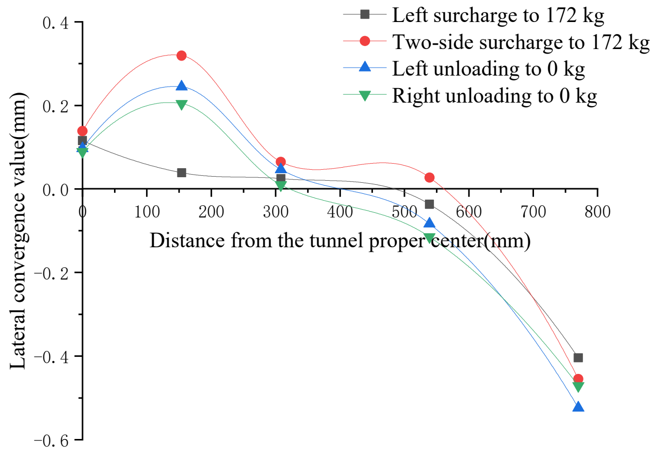

Figure 16. Variation in the lateral convergence of each measurement point in the tunnel under different surcharge conditions for Case 4.

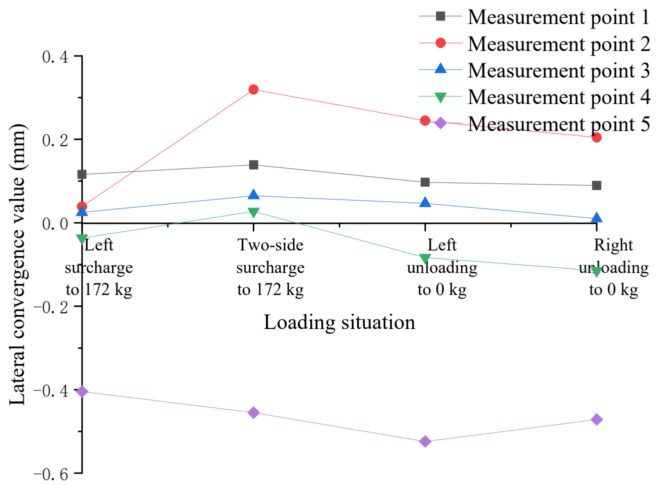

Figure 17. Variation in the lateral convergence of the tunnel under different surcharges for each measurement point in Case 4.

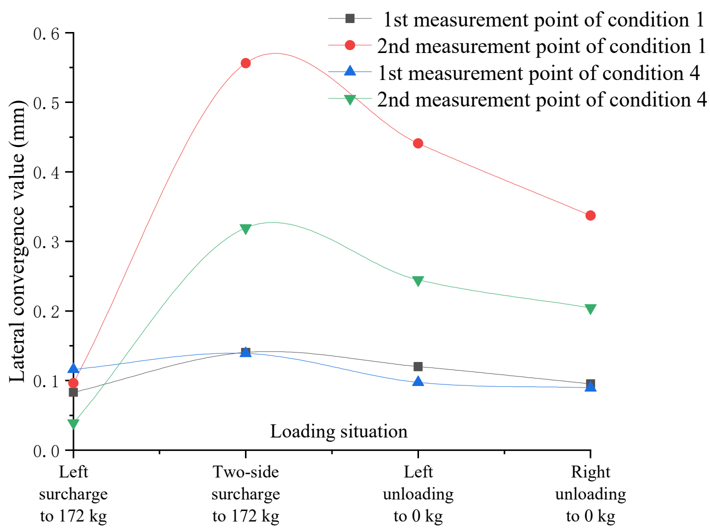

Figure 18. Variation of transverse convergence with surcharge for the 1st and 2nd measurement points in Case 2 and Case 4.

Analysis of Figures 16–18 shows the following:

(1) In the wet sand, the maximum transverse convergence value of the tunnel occurs at measurement point 2 when the eccentric surcharge on two sides of the tunnel is 172 kg, which is consistent with the case of dry sand in soil under the same conditions, but the maximum transverse convergence value of the tunnel in the wet sand is 0.3193 mm—only 57.4% of the transverse convergence of the tunnel in the dry sand under the same conditions—indicating that under the same test conditions, compared with the dry sand, the maximum transverse convergence of the tunnel in the wet sand is significantly reduced.

(2) The unloading of either side in wet sand can effectively reduce the lateral convergence value of the tunnel when two sides are surcharged, which is consistent with the performance under dry sand soil. Taking measurement point 2 as an example, after unloading the two-sided surcharge, the transverse convergence value is reduced from the maximum 0.3193 mm to 0.2044 mm, representing a reduction of 36.0%.

(3) The lateral convergence value of measurement point 5 is obviously different from that of the other measurement points, which is influenced by the boundary effect of the model test.

3.2.2. Effect on Ground Settlement

The variation in ground shift under different surcharges for Case 4 is shown in Figure 19, and the variation in the ground shift of each measurement point under different surcharges for Case 4 is shown in Figure 20, where the positive values of ground shift represent augmentation and the negative values represent settlement.

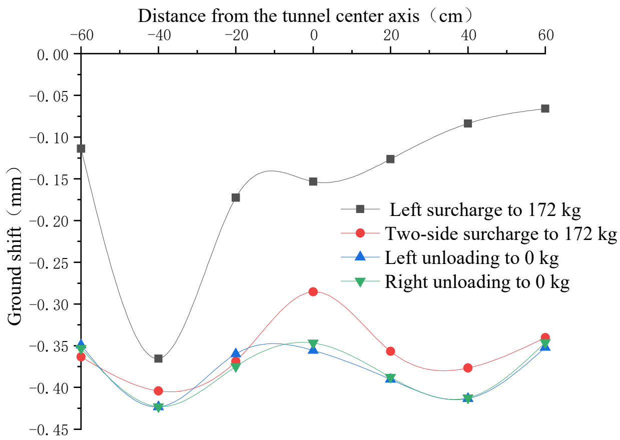

Figure 19. Variation in ground shift under different surcharges for Case 4.

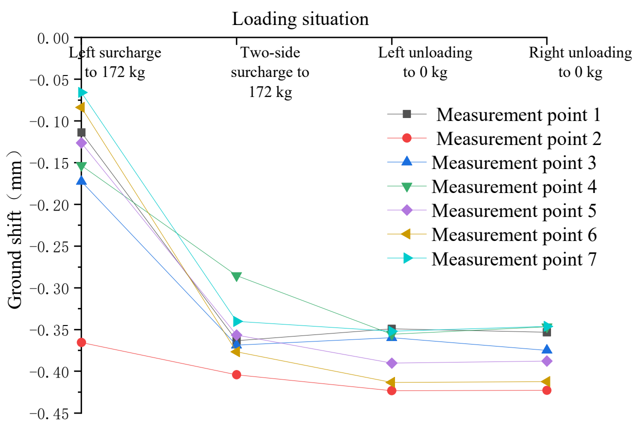

Figure 20. Variation in ground shift at each measurement point under different surcharges for Case 4.

Combining Figures 11, 19 and 20, the following can be seen:

(1) When the soil is wet sand, the peak of ground settlement on the left and right sides occurs when the surcharge on the right side is 172 kg and the unloading on the left side is completed, while the effect of unloading on the mitigation of ground settlement is not obvious and is the same as when the soil is dry sand.

(2) Under two-sided surcharge in wet sand, the peak of ground settlement on the two sides is not significant; the ground settlement caused by surcharge in wet sand is significantly smaller than that caused by surcharge in dry sand under the same conditions, and the peak ground settlement on the left and right sides in wet sand is 0.4232 mm. The peak settlement in wet sand is 0.4232 mm and 0.4133 mm, which is only 51.1% and 38.2% of the peak settlement on the left and right sides with dry sand soil, respectively.

3.2.3. Effect on Additional Surrounding Pressure

The additional envelope pressure of the positive central section of the tunnel in Case 4 is shown in Figure 21, where the positive values of the additional envelope pressure represent the pressure and the negative values represent the tension.

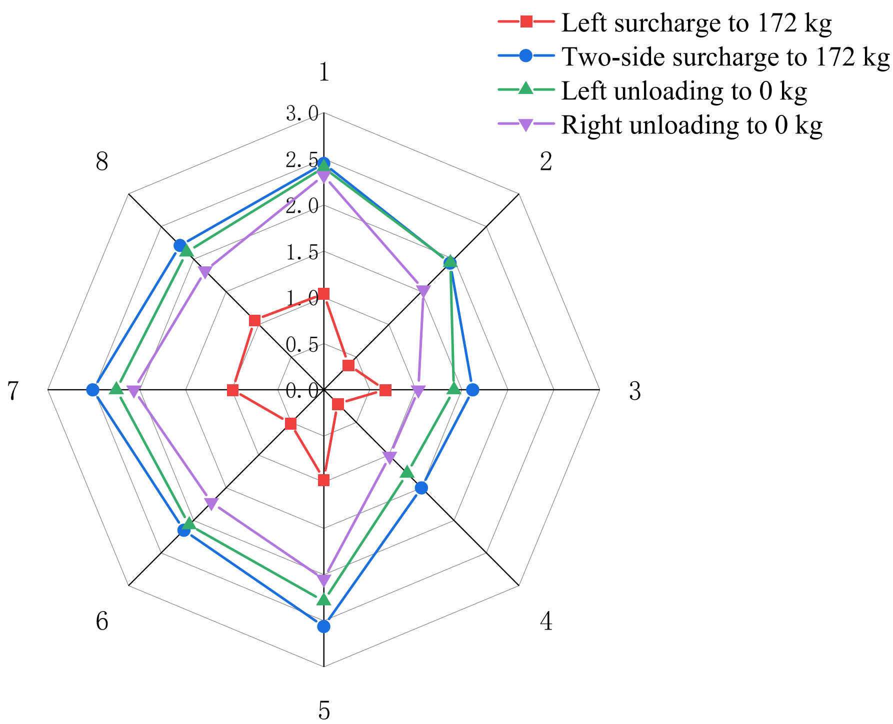

Figure 21. Variation in additional surrounding pressure under different surcharges for Case 4 (unit: kPa).

Combining Figures 2 and 21, the following can be seen:

(1) The overall additional envelope pressure in the tunnel in wet sand is significantly larger than that in the tunnel in dry sand under the same conditions when the left surcharge is offset by 0.4 m, which is exactly the opposite of the overall additional envelope pressure in the tunnel in wet sand which, according to the literature, is significantly smaller than that in the tunnel in dry sand under the same conditions when the tunnel is surcharged directly above [8]. This is because the stress σ contours are flatter when the soil is wet sand, and the stress decreases slowly with the increase in the bias distance D. When the soil is dry sand, the stress σ contours are relatively long and thin, and the stress σ decreases rapidly with the increase in the deflection distance D. The stress σ contours for dry and wet sand under two-sided surcharge for Case 2 and Case 4 are shown schematically in Figures 22 and 23, respectively.

(2) In the wet sand, unloading can reduce the additional surrounding pressure of the tunnel to some extent, but the effect is obviously worse than that of dry sand unloading under the same conditions. Taking measurement point 1 as an example, in Case 2, the additional surrounding pressure is 2.3129 kPa when the two-sided surcharge is 172 kg, and the additional surrounding pressure is 1.0271 kPa after the two-sided surcharge is unloaded to 0 kg, with a reduction rate of 55.6%. In Case 4, the additional surrounding pressure is 2.4497 when two-sided surcharge is 172 kg, and the additional surrounding pressure is 1.0271 kPa after the two-sided surcharge is unloaded to 0 kg. kPa, while it is 2.3215 kPa after unloading to 0 kg on both sides, which is only a 5.2% decrease. This is because there is a lag in the reduction in the additional surrounding pressure of the tunnel after unloading in the wet sand condition due to the difference in soil, and a lag in the reduction in the additional surrounding pressure of the tunnel after unloading above the tunnel in the soft clay condition was also found in the literature [6].

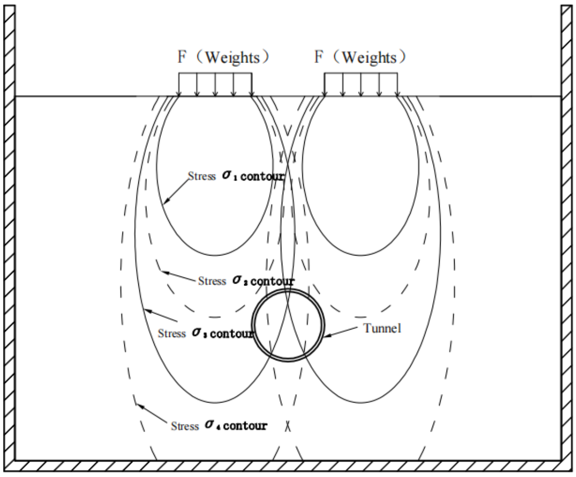

Figure 22. Stress σ contour of dry sand at surcharge on two sides.

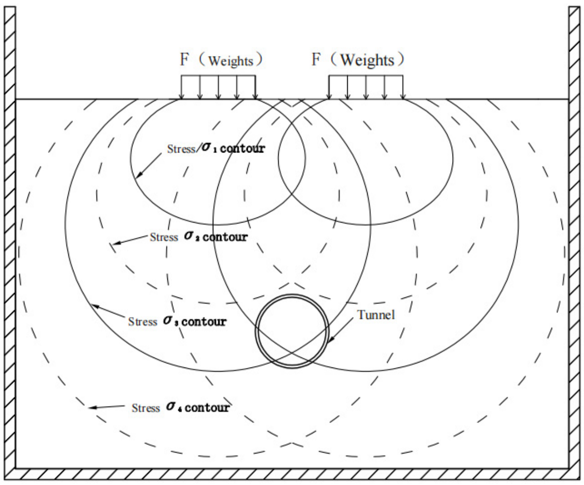

Figure 23. Stress σ contour of wet sand at surcharge on two sides.

3.2.4. Influence on Additional Soil Pressure at the Bottom of the Tunnel

The variation in the additional soil pressure at the bottom of the tunnel under different surcharge conditions is shown in Figure 24, where the positive values of the additional soil pressure represent compression and the negative values represent tension.

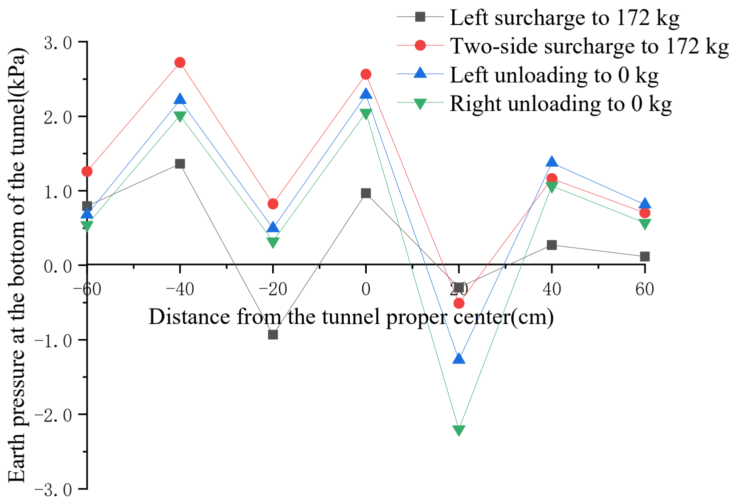

Figure 24. Variation in additional soil pressure at the bottom of the tunnel under different surcharges in Case 4.

Analysis of Figure 24 shows the following:

(1) Unloading can reduce the additional soil pressure of the tunnel subsoil to a certain extent, from the process of surcharge to 172 kg on two sides to the completion of unloading on both sides; the maximum reduction in the additional soil pressure of the tunnel subsoil is 0.7094 kPa, which occurs at measurement point 2 at −40 cm from the tunnel center; the maximum reduction in additional soil pressure of the tunnel subsoil is 61.0%, which occurs at measurement point 3 at −20 cm from the tunnel center. The maximum reduction in soil pressure is 61.0%, which occurs at measurement point 3 at −20 cm from the center of the tunnel.

(2) During the process from surcharge to 172 kg on two sides to complete unloading to 0 kg on the left side (i.e., surcharge is still 172 kg on the right side), the additional soil pressure at measurement point 6 at 40 cm from the tunnel center increases instead of decreasing, and the increase reaches 0.2134 kPa, which is an increase of 18.35%. The local unloading of the surcharge will lead to an increase in the accumulated additional soil pressure of the tunnel subsoil, and the unloading sequence will affect the distribution of the additional soil pressure of the tunnel subsoil.

(3) When the two-sided surcharge is 172 kg, the surcharge on both sides is symmetrical along the longitudinal axis of the tunnel, but the accumulated additional soil pressure of the tunnel's subgrade is not completely symmetrical, which indicates that the surcharge order will affect the distribution of the additional soil pressure of the tunnel subgrade.

(4) When the two-sided surcharge is 172 kg, the additional soil pressure of the tunnel subgrade shows three peaks, one of which occurs at measurement point 4 at the bottom of the tunnel, probably because the stress concentration occurs here, resulting in a high additional soil pressure; two of these peaks occurred at measurement points 2 and 6 directly below the surcharge, and the range of the two-sided surcharge was 0.4 m × 0.4 m, but the difference between the accumulated additional soil pressure of the tunnel subsoil directly below the surcharge and the additional soil pressure of the tunnel subsoil below the edge of the surcharge was great, which was related to the characteristics of the sand soil itself—under the action of loading, the sand particles at the edge of the substrate (i.e., bearing plate) are very easy to extrude toward the lateral direction, so the middle of the substrate (i.e., bearing plate) must provide a greater balance of the reaction force, so that the reaction force distribution is inverted "convex"; specifically, refer to Figure 25.

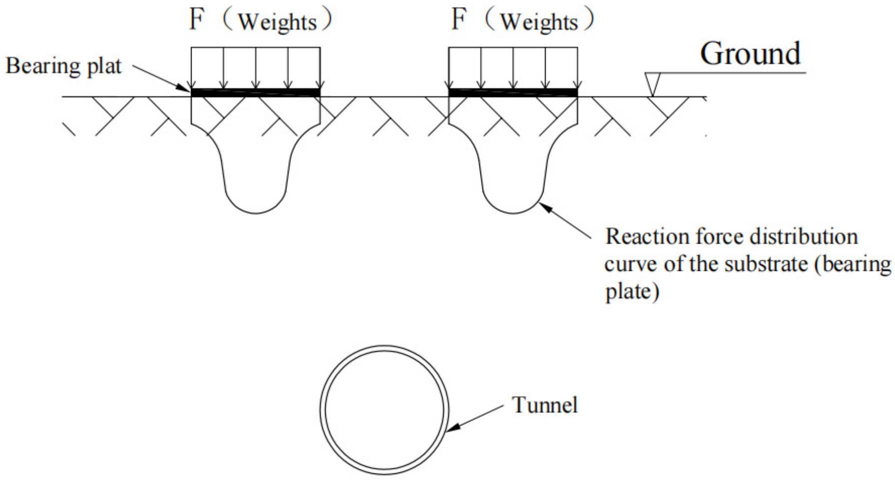

Figure 25. The base (the bottom of the pressure plate) of the reaction force distribution diagram.

4. Conclusions

(1) The location of the maximum transverse convergence value of the existing shield tunnel is related to the location of the surcharge, because the location of the load on the two sides of the tunnel is different, resulting in the combined force of the two sides of the load on the tunnel being different. With the surcharge on two sides of the tunnel, as the left surcharge's offset position increases from 0.2 m to 0.6 m, the tunnel's transverse convergence value will first increase and then become smaller, and the transverse convergence value will decrease rapidly after the surcharge's offset reaches a certain degree.

(2) In dry sand soil, as the left surcharge's offset position increases from 0.2 m to 0.6 m, the additional pressure of the tunnel decreases sharply; after one side of the tunnel is surcharged, if the other side continues to surcharge, it will lead to a continued increase in the surrounding pressure, and when the two-sided surcharge reaches 172 kg, the local additional pressure of the tunnel increases by more than 100%. After unloading, the additional pressure in most of the tunnel will still exist to some extent, and the residual proportion of additional pressure will be related to the offset position of the surcharge—the more distant the surcharge position, the higher the residual proportion of additional pressure.

(3) Under the same test conditions, compared with dry sand, the maximum value of lateral convergence of the tunnel in wet sand is significantly reduced, the peak value of ground settlement on both sides is not significant, the amount of ground settlement caused by the surcharge is significantly smaller, and the mitigating effect of unloading on ground settlement and the reduction in additional pressure are not obvious.

(4) When the left surcharge is offset by 0.4 m, the additional envelope pressure of the tunnel in wet sand is generally significantly larger than that of the tunnel in dry sand under the same conditions because, due to the differences in soil properties, the stress σ contours are flatter when the soil is wet sand, and the stress decreases slowly with the increase in the offset distance D. When the soil is dry sand, the stress σ contours are relatively long and thin, and the stress σ decreases rapidly with the increase in the deflection distance D.

(5) In the wet sand soil, the additional earth pressure of the tunnel's subsoil presents three peaks when the surcharge to 172 kg on both sides, one of which occurs at measurement point 4 at the bottom of the tunnel, which may be due to the stress concentration occurring here, resulting in a high additional earth pressure. The other two occur at measurement point 2 and measurement point 6 directly below the surcharge, and the range of the two-sided surcharge is 0.4 m $\times$ 0.4 m, but the accumulated additional soil pressure of the tunnel subsoil directly below the surcharge and the additional soil

pressure of the tunnel subsoil below the edge of the surcharge are very different, due to the characteristics of the sand soil itself.

Only one kind of wet sand with a specific water content was used in this model test, and the effect of water content in the sand soil was not considered, which still needs further investigation in future tests and research.

Author Contributions: Methodology and guidance, G.W.; data curation, editing, and analysis, P.X.; analysis and project administration, H.J.; supervision and interpretation of data, D.S.; review and revision, F.X.; supervision and translation, H.G. All authors have read and agreed to the published version of the manuscript.

Funding: This research was funded by the Basic Public Welfare Research Projects in Zhejiang Province, grant number LGF22E080012; and the National Natural Science Foundation of China, grant number 52178399.

Institutional Review Board Statement: Not applicable.

Informed Consent Statement: Not applicable.

Data Availability Statement: Not applicable.

Conflicts of Interest: The authors declare no conflict of interest.

References

1. Liu, T.J.; Chen, S.W.; Ye, Z.W. Analysis of disease and structural safety of shield tunnel under accidental surface surcharge. *J. Railw. Eng. Soc.* **2019**, *36*, 67–73.
2. Lu, P.Y.; Wang, M.L.; Yang, J.M. Influences of surface surcharge on the deformation of shield tunnel in soft ground area. *Build. Struct.* **2019**, *49*, 999–1003.
3. Ma, Z.Z.; Luo, Z.H.; Zhang, J.; Xin, H.H. Study on influence of ground surcharge on deformation of subway shield tunnel. *Mod. Tunn. Technol.* **2018**, *55*, 573–578.
4. Lai, H.R.; Huang, C.Y.; Liu, X.Z.; Tu, X.B.; Xie, J.; Sang, Y.L. Analysis on the effects of overloading on the mechanical properties of tunnel structures in the silty ground. *Mod. Tunn. Technol.* **2018**, *55*, 88–96.
5. Shao, H.; Huang, H.W.; Zhang, D.M.; Wang, R.L. Case study on repair work for excessively deformed shield tunnel under accidental surface surcharge in soft clay. *Chin. J. Geotech. Eng.* **2016**, *38*, 1036–1043.
6. Xiang, P.F.; Wei, G.; Zhang, S.M.; Cui, Y.L.; Guo, H.F. Model test on the influence of surcharge, unloading and excavation of soft clay soils on shield tunnels. *Symmetry* **2021**, *13*, 2020. [CrossRef]
7. Wei, G.; Zhang, S.M.; Xiang, P.F. Model test study on the influence of ground surcharges on the deformation of shield tunnels. *Symmetry* **2021**, *13*, 1565. [CrossRef]
8. Zhang, S.M. Research on the Influence of Ground Load on the Force and Deformation of Shield Tunnel. Master's Thesis, Anhui University of Science and Technology, Huainan, China, 2021.
9. Liang, F.Y.; Fang, Y.Q.; Yuan, Q.; Li, J.P. Experimental study of the influence of surface surcharge on tunnel lateral deformation in soft and hard soil. *J. Tongji Univ. (Nat. Sci.)* **2021**, *49*, 322–331+430.
10. Sun, H.S.; Zhou, T.; Dong, Y.; Chen, Y.D.; Zhang, J.H. Effect of ground surcharge on the deformation of an existing tunnel. *Chin. J. Undergr. Space Eng.* **2019**, *15*, 900–907+913.
11. Wu, Q.; Du, S.J. Model test on influence of ground heaped load on existing shield tunnel structure. *Chin. J. Undergr. Space Eng.* **2014**, *10*, 57–66.
12. Atkinson, J.H.; Potts, D.M. Stability of a shallow circular tunnel in cohesionless soil. *Geotechnique* **1977**, *27*, 203–215. [CrossRef]
13. Liu, J.H.; Yan, Y.Z.; Zhang, Q.; Bian, R.; He, L.; Ye, G.L. Centrifugal test and numerical analysis of impact of surface surcharge on existing tunnels. *J. Shanghai Jiao Tong Univ.* **2022**, *56*, 886–896.
14. Zhang, F.; Yu, Z.H.; Wang, D.S.; Wang, L.L.; Mei, H.J.; Hu, S.S. Analysis of shield segment deformation induced by ground surcharge. *Sci. Technol. Eng.* **2022**, *22*, 8908–8915.
15. Xie, J.C.; Wang, J.C.; Huang, W.M. Nonlinear structural analysis on cracking behavior of shield tunnel segment under surface loading. *J. Railw. Sci. Eng.* **2021**, *18*, 162–171.
16. Bian, R.; Liu, H.Q.; Chen, F.; Wu, B.; He, L.; Ye, G.L. Numerical analysis on the influence of ground heaped load on tunnel considering small strain stiffness of soil. *Sci. Technol. Eng.* **2020**, *20*, 7407–7412.
17. Wei, G.; Hong, W.Q.; Wei, X.J.; Jiang, J.Q. Deformation law and control limit of shield tunnel cross-section under eccentric surcharge load. *J. Cent. South Univ.* **2020**, *51*, 750–757.
18. Sun, L.W.; Qin, J.S.; Hong, Y.; Wang, L.Z.; Zhao, C.J.; Qin, X. Shield tunnel segment and circumferential joint performance under surface surcharge. *J. Zhejiang Univ. (Eng. Sci.)* **2017**, *51*, 1509–1518.

19. Lu, D.Y.; Xu, G.W.; Wang, S.M. Effects of material damage and structural characteristics on tunnel shield during loading and unloading. *J. Southwest Jiaotong Univ.* **2017**, *52*, 1104–1112.
20. Papanikolaou, V.K.; Kappos, A.J. Practical nonlinear analysis of unreinforced concrete tunnel linings. *Tunn. Undergr. Space Technol.* **2014**, *40*, 127–140. [CrossRef]
21. Doležalová, M. Tunnel complex unloaded by a deep excavation. *Comput. Geotech.* **2001**, *28*, 469–493. [CrossRef]
22. Wang, M.; Gan, X.L.; Du, W.; Yu, J.L.; Gong, X.N. Effects of surface surcharge on existing tunnel considering soil stiffness degradation. *Chin. J. Undergr. Space Eng.* **2021**, *17*, 1965–1971+1979.
23. Zhang, Z.G.; Zhang, Y.B.; Zhang, C.P.; Wang, Z.W.; Pan, Y.T. Time-domain solution for soil feedback induced by shield tunneling in viscoelastic strata considering influences of surcharge loading. *Chin. J. Geotech. Eng.* **2021**, *43*, 34–42.
24. Liang, F.Y.; Yuan, Q.; Li, J.P.; Zhang, S.X. Influences of soil characteristics on longitudinal deformation of shield tunnels induced by surface surcharge. *Chin. J. Geotech. Eng.* **2020**, *42*, 63–71.
25. Wei, G.; Hong, W.Q.; Wei, X.J.; Lin, X.B.; Wang, L.Z. Theoretical calculations of transverse force on shield tunnel caused by eccentric load. *J. Cent. South Univ. (Sci. Technol.)* **2019**, *50*, 1645–1654.
26. Wei, G.; Yu, G.H.; Hong, W.Q. Study on calculation of shield tunnel shearing dislocation platform deformation due to adjacent ground stacked load. *J. Cent. South Univ. (Sci. Technol.)* **2018**, *49*, 1775–1783.
27. Wei, X.J.; Hong, W.Q.; Wei, G.; Yu, G.H. Rotation and shearing dislocation deformation of subway tunnels due to adjacent ground stack load. *Chin. J. Rock Mech. Eng.* **2018**, *37*, 1281–1289.
28. Kang, C.; Mei, G.X.; Liang, R.Z.; Wu, W.B.; Fang, Y.X.; Ke, Z.B. Analysis of the longitudinal deformation of existing shield tunnel induced by temporary surface surcharge. *Rock Soil Mech.* **2018**, *39*, 4605–4616.
29. Huang, H.W.; Zhang, D.M. Resilience analysis of shield tunnel lining under extreme surcharge: Characterization and field application. *Tunn. Undergr. Space Technol.* **2016**, *51*, 301–312.
30. Kentaro, Y.; Andrei, V.L.; Daniel, W.W.; Scott, W.S.; Andrew, J.A. Stability of dual circular tunnels in cohesive-frictional soil subjected to surcharge loading. *Comput. Geotech.* **2013**, *50*, 41–54.
31. Kentaro, Y.; Andrei, V.L.; Daniel, W.W.; Scott, W.S.; Andrew, J.A. Stability of a circular tunnel in cohesive-frictional soil subjected to surcharge loading. *Comput. Geotech.* **2011**, *38*, 504–514.